The heme iron coordination of unfolded ferric and ferrous cytochrome c in neutral and acidic urea solutions. Spectroscopic and electrochemical studies

ARTICLE *in* BIOCHIMICA ET BIOPHYSICA ACTA · JANUARY 2005

Impact Factor: 4.66 · DOI: 10.1016/j.bbapap.2004.09.013 · Source: PubMed

9 AUTHORS, INCLUDING:

Milan Fedurco
Michelin Switzerland
54 PUBLICATIONS **2,871** CITATIONS
SEE PROFILE

Chiara Indiani
Manhattan College
29 PUBLICATIONS **1,092** CITATIONS
SEE PROFILE

Giulietta Smulevich
University of Florence
187 PUBLICATIONS **4,591** CITATIONS
SEE PROFILE

Erik Sedlák
Pavol Jozef Šafárik University in Košice
53 PUBLICATIONS **908** CITATIONS
SEE PROFILE

Available online at www.sciencedirect.com

SCIENCE DIRECT

Biochimica et Biophysica Acta 1703 (2004) 31–41

BIOCHIMICA ET BIOPHYSICA ACTA BBA

http://www.elsevier.com/locate/bba

The heme iron coordination of unfolded ferric and ferrous cytochrome *c* in neutral and acidic urea solutions. Spectroscopic and electrochemical studies

Milan Fedurco[a,*], Jan Augustynski[a], Chiara Indiani[b], Giulietta Smulevich[b], Marián Antalík[c], Mikuláš Bánó[c], Erik Sedlák[d], Mary C. Glascock[e], John H. Dawson[e]

[a]*Department of Chemistry, University of Geneva, 30 quai Ernest Ansermet, CH-1211 Geneva, Switzerland*
[b]*Department of Chemistry, University of Florence, Via della Lastruccia 3, 50019 Sesto Fiorentino (F1), Italy*
[c]*Department of Biophysics, Institute of Experimental Physics, Slovak Academy of Sciences, Watsonova 47, 043 53 Košice, Slovakia*
[d]*Department of Biochemistry, Faculty of Science, P.J. Safárik University, Moyzesova 11, 041 54 Košice, Slovakia*
[e]*Department of Chemistry and Biochemistry, University of South Carolina, Columbia, SC 29208, USA*

Received 26 May 2004; received in revised form 20 August 2004; accepted 14 September 2004
Available online 30 September 2004

Abstract

The heme iron coordination of unfolded ferric and ferrous cytochrome *c* in the presence of 7–9 M urea at different pH values has been probed by several spectroscopic techniques including magnetic and natural circular dichroism (CD), electrochemistry, UV–visible (UV–vis) absorption and resonance Raman (RR). In 7–9 M urea at neutral pH, ferric cytochrome *c* is found to be predominantly a low spin bis–His-ligated heme center. In acidic 9 M urea solutions the UV–vis and near-infrared (NIR) magnetic circular dichroism (MCD) measurements have for the first time revealed the formation of a high spin His/H_2O complex. The pK_a for the neutral to acidic conversion is 5.2. In 9 M urea, ferrous cytochrome *c* is shown to retain its native ligation structure at pH 7. Formation of a five-coordinate high spin complex in equilibrium with the native form of ferrous cytochrome *c* takes place below the pK_a 4.8. The formal redox potential of the His/H_2O complex of cytochrome *c* in 9 M urea at pH 3 was estimated to be −0.13 V, ca. 100 mV more positive than $E^{\circ\prime}$ estimated for the bis–His complex of cytochrome *c* in urea solution at pH 7.

Keywords: Cytochrome *c*; Urea; Magnetic circular dichroism; Raman spectroscopy

1. Introduction

During the last decade, cytochrome *c* (cyt *c*) has moved to the center of the scientific attention mainly due to the discovery that it is able to leave the mitochondria and function as a death messenger in programmed cell death [1–3]. In addition, horse heart cyt *c* has become one of the most important model molecules in protein folding studies [4–16]. The single tryptophan residue in this metalloprotein serves as a built-in fluorescent label and very useful indicator of conformational changes observed in highly concentrated solutions of urea, or guanidinium hydrochloride (GdnHCl). Since the heme group in cyt *c* is covalently bonded to the polypeptide chain, optical transitions in the UV–visible (UV–vis) and near-infrared (NIR) regions of the spectra are sensitive to denaturant-induced ligand-exchange reactions and to accompanying relaxation of the strain imposed on the heme by the protein. The progress of cyt *c* denaturation and/or its refolding can then be readily monitored by several spectroscopic techniques.

Abbreviations: cyt *c*, cytochrome *c*; UV–vis, UV–visible; GdnHCl, guanidine hydrochloride; MCD, magnetic circular dichroism; CD, circular dichroism; NHE, normal hydrogen electrode; NIR, near-infrared; RR, resonance Raman; CT, charge transfer

* Corresponding author. Tel.: +41 022 379 3114; fax: +41 022 379 6830.
E-mail address: milan_fedurco@freesurf.ch (M. Fedurco).

1570-9639/$ - see front matter © 2004 Elsevier B.V. All rights reserved.
doi:10.1016/j.bbapap.2004.09.013

In general, unfolding of cyt *c* can be pictured as the progressive breaking of hydrogen bonds in the protein interior and gradual exposure of amino acid residues, normally buried in the protein interior, to solvent and denaturant molecules. The ionic character of GdnHCl and lower dielectric constant of its solutions in water could at least in part explain its ability to unfold cyt *c* at lower concentrations (<5 M) than urea. On the other hand, urea is known to efficiently solubilize aromatic amino acid residues, which become progressively exposed to the solvent during the unfolding process [17]. Circular dichroism (CD) studies have shown that the ordered helical structure of cyt *c* gradually disappears with increasing concentration of urea and the protein adopts a random-like structure in 9 M urea [10]. At present, it is not known how much of the residual helical structure is preserved in what is called "unfolded cyt *c*″. On the other hand, it is becoming progressively clearer how the axial ligation in unfolded cyt *c* stabilizes the protein against refolding.

Recent NMR studies of the ferric protein have provided direct experimental evidence concerning the identity of the amino acid ligands bound to the heme iron as a function of denaturant concentration in neutral urea solutions [14,15]. It is interesting in this respect that Russell et al. [14,15] noticed significant differences in heme ligation in highly concentrated urea solutions as compared to GdnHCl. While one unfolding intermediate of cyt *c* and one unfolded species were detected by NMR spectroscopy in urea, two unfolding intermediates with His/Lys ligation and two unfolded species with His/His ligation were detected in GdnHCl solutions [15]. The following distribution of species was found for ferric cyt *c* in 7 M urea (pH 7) from 2D-NMR (NOESY) measurements: 33% His/Met, 20% His/His, 16% His/Lys, the remaining being NMR silent species [14].

Surprisingly, in more concentrated urea solutions (c_{urea}=7–9 M), more than 50% of the cyt *c* is present in a form that is unobservable by NMR. This latter form of cyt *c* was proposed by Russell et al. to be a bis–His complex in which one of the histidine ligands has a highly disordered orientation. Clearly, a limitation of these NMR experiments was the inability to study all of the species of cyt *c* present under a given set of conditions. In the present study, we have investigated the heme iron coordination structure of ferric as well as ferrous urea-denatured cyt *c* with resonance Raman (RR) spectroscopy, natural and magnetic circular dichroism (MCD) and electrochemistry from neutral pH down to pH 2. Identification of the axial ligands to the central heme iron in the urea-denatured protein is of considerable relevance to the numerous protein folding studies that have involved cyt *c* [4–16]. The combination of RR and MCD spectroscopy provides a powerful way to probe the coordination structure of heme iron centers in proteins, including the establishment of the spin state and identification of the axial ligands [18,19].

2. Materials and methods

Horse heart cyt *c* (type VI, Sigma) was fully oxidized prior to use by treatment with excess potassium ferricyanide (Fisher) [20]. Sodium hydrosulfite (dithionite) and sodium borohydride were obtained from Sigma (Germany), deuterium oxide from Cambridge Isotopes, and urea from Bio-Rad Laboratories (USA), Aldrich (Germany), or Fisher (USA). The urea concentration was determined from its refractive index [21]. Double-distilled water was used in all experiments. The concentration of ferric cyt *c* was determined by using $\varepsilon_{409\ nm}$=106 $mM^{-1} \cdot cm^{-1}$ [22]. The concentration of ferrous cyt *c* was determined after re-oxidation with ferricyanide. Ferrous cyt *c* was prepared by addition of aqueous sodium dithionite or crystalline $NaBH_4$. Excess dithionite was removed by G-25 Sephadex gel filtration. Re-oxidation of the ferrous cyt *c* under acidic conditions (pH<4.8) was found to be very fast.

2.1. UV–vis absorption and CD measurements

UV–vis absorption spectra were recorded at 25 °C with a Cary 5 spectrophotometer. Spectrophotometric titrations were performed on a Shimadzu UV-3000 spectrophotometer. Phosphate buffer (in a cuvette) containing cyt *c* was deoxygenated with argon (99.96%) that had been passed through an alkaline pyrogallol solution (5% w/v) to scavenge trace oxygen. CD measurements were conducted at 20 °C using an OLIS Cary-16 spectropolarimeter (USA). Samples were prepared in 10 mM phosphate buffer solution containing 16–19 μM cyt *c* ±9.0 M urea. The time between the preparation of the sample and recording the spectrum was always shorter that 100 s, during which time less than 5% oxidation was observed. During the CD measurements, the cuvette was continuously purged with nitrogen. CD spectra of ferric cyt *c* are averages of three to eight scans. Single CD spectra of ferrous cyt *c* were recorded in the range 190–350 nm to avoid any effects of oxidation on the ferrous cyt *c*. CD spectra of ferrous cyt *c* are averages of three scans in the range 380–450 nm, where an excess of solid crystalline sodium dithionite was added immediately before each measurement (dithionite strongly absorbs below 380 nm). Cuvettes of 1 and 5 mm were used for measurements in the regions 190–250 and 250–450 nm, respectively. Typically, a time constant of 1 s, bandwidth of 1.0–1.5 nm and 200 points/100 nm were used.

2.2. MCD

Protein samples were prepared in 10 mM potassium phosphate in deuterium oxide. The pH was corrected according to pD=pH+0.4 [23] and adjusted with DCl and KOD. The imidazole complex of ferric cyt *c* was prepared as previously described [24–26]. NIR and UV–visible MCD/CD data were recorded at 4 °C with JASCO J200 and J600 spectropolarimeters, respectively, each equipped

with a JASCO MCD-1B electromagnet operated at 1.41 T. Both spectropolarimeters were interfaced to an IBM PC for data acquisition.

2.3. RR spectroscopy

The protein was dissolved in 0.1 M potassium phosphate buffer at pH 7.0. Solution pH was adjusted with dilute HCl. Cyt *c* concentration was typically 10–40 μM and an excitation wavelength of 406.7 nm from a Kr^+ laser (Coherent, Innova 90/K) was used [27]. The RR spectra were calibrated with indene and CCl_4 as standards to an accuracy of ± 1 cm^{-1}. Relative intensities of the high frequency RR bands of cyt *c* were normalized on the ν_4 band (not shown in the figures). Absorption spectra, recorded with a Cary 5 spectrophotometer, were measured both prior to and after RR measurements; no degradation was observed.

2.4. Electrochemistry

All solutions were freshly made from reagent-grade chemicals and high purity water (18.2 MΩ. cm resistivity, Millipore). Cyclic voltammetric measurements were performed in deaerated solutions, under argon, at 22 ± 1 °C in a two-compartment glass cell using the portable PC-based Eco-Tribo Polarographic Analyser in a three-electrode configuration (Polaro-Sensors, Prague). All potentials were measured against an $Ag/AgCl/Cl^-$ reference electrode and are reported versus normal hydrogen electrode (NHE). A platinum counter-electrode (large area Pt grid) was separated from a working electrode by a ceramic separator. A cross-section of the Ag(111) low-index single crystal rod oriented with 0.5° accuracy (Metal Crystals and Oxides, Ltd.), served as working electrode (3 mm in diameter). The electrode surface was prepared by polishing mechanically with fine emery paper and then with suspensions of 1.0 and 0.3 μm alumina powders. Alumina was removed from the electrode surface via gentle sonication in an ultrasonic bath and washing with a copious amount of distilled water. Before the measurements, the electrode surface was cleaned by cycling the potential into the hydrogen evolution region in 0.1 M $NaClO_4$. The pH of the 0.01 M phosphate buffer/0.1 M $NaClO_4$ solution was adjusted with dilute $HClO_4$. Cyclic voltammograms for cyt *c* were recorded on 2-mercaptoethanol-modified Ag(111) electrode using the polarization rate (scan rate) of 100 mV/s.

3. Results and discussion

3.1. Spectroscopy of ferric cytochrome c in urea

3.1.1. UV–vis absorption

At pH 7.0, increases in the urea concentration cause progressive changes in the UV–vis absorption spectra of ferric cyt *c* (Fig. 1). The Soret and Q bands blue-shift, and the charge transfer (CT) band at around 695 nm disappears. In 9 M urea, the spectrum of cyt *c* in the visible region closely resembles that of the bis–His cyt *c″* at pH 7.0 [27], consistent with the replacement of the axial Met-80 by a His ligand. The absorption spectrum of ferric cyt *c* in both the presence and absence of 9 M urea changes considerably upon lowering the pH. At pH 2.0, a new species appears that is characterized by a Soret absorption band at 396–394 nm, Q bands at about 495 and 530 nm, and a new CT1 band at 620–618 nm. The changes induced by lowering the pH are consistent with an increase of high spin species at the expense of the low spin heme observed at higher pH. The amount of the high spin species present at pH 2 in 9 M urea is slightly higher than in the absence of the urea. On the basis of the intensity changes of the band at 620 nm (Fig. 2), or in the Soret absorption band (data not shown), induced by lowering the pH, a pK_a of 5.2 was determined, which is nearly identical to that found for the protonation of His-33 [12,28].

3.1.2. CD

The CD spectrum of ferric cyt *c* is rich in detail over the entire spectral region reflecting the contributions from transitions arising from various chromophores (Fig. 3). Since the origins of most of these transitions are well characterized, the investigation of variations of their rotatory strength significantly aid in interpretation of the conformational implications for the protein. The far-UV (190–250 nm) CD spectrum is a sensitive probe for protein secondary structure. The CD spectrum of ferric cyt *c* in solution shows

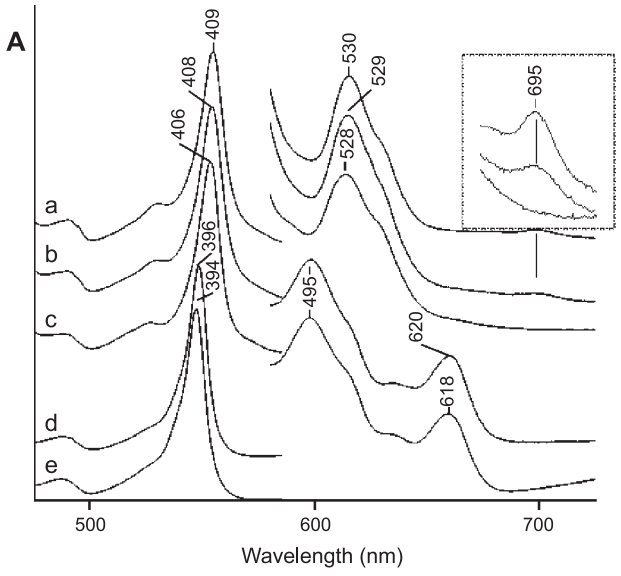

Fig. 1. UV–vis absorption spectra of ferric cyt *c* in 10 mM phosphate: (a) pH 7.0, no urea; (b) pH 7.0, 6 M urea; (c) pH 7.0, 9 M urea; (d) pH 2.0, 9 M urea; (e) pH 2.0, no urea. The 450–750 nm region has been expanded 7-fold. The inset shows the 650–750 nm region of the a, b, and c spectra which have been expanded 40-fold.

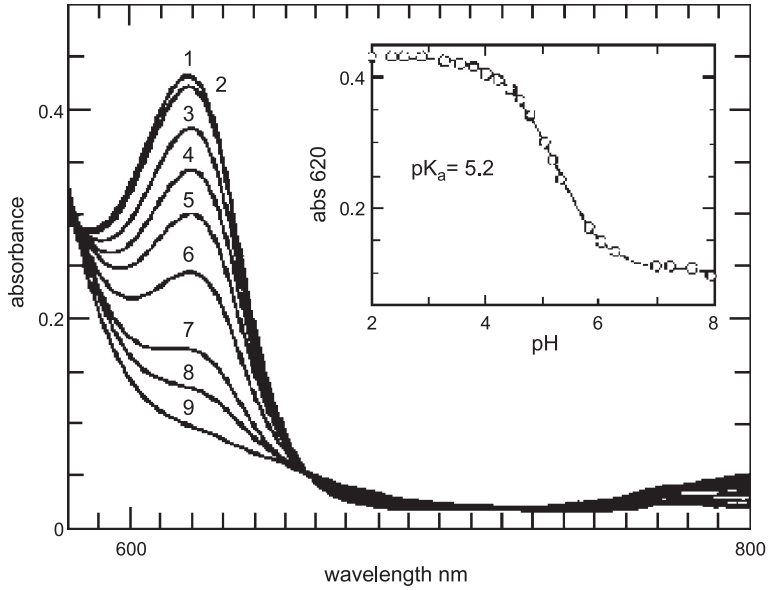

Fig. 2. The pH dependence of the intensity of the CTI band at 620 nm for ferric cyt *c* in 10 mM phosphate/9 M urea. (1) pH 2.6; (2) pH 3.4; (3) pH 4.1; (4) pH 4.5; (5) pH 5.0; (6) pH 5.5; (7) pH 5.9; (8) pH 7.3; (9) pH 7.8. The inset shows the absorbance versus pH data and the calculated curve for a single protonation step with observed apparent p*K* at 5.2.

the typical features of a α-helical protein structure with the 222 and 208 nm dichroic bands (Fig. 3) that are predominantly associated with α-helical amide transitions [29–31].

CD in the near-UV (250–350 nm) and Soret (350–450 nm) regions reflects changes in the tertiary structure of the protein that affect the environment of aromatic side chains and the heme pocket. The CD spectrum of ferric cyt *c* in the near-UV region is characterized by two sharp minima at 282 and 288 nm (Fig. 3), assigned previously to transitions linked with the Trp-59 side chain [31,32]. The band centered around 251 nm reflects a contribution from tyrosine side chains, and the 262 nm band appears to be associated with the heme [30,31].

Ferric cyt *c* exhibits a characteristic CD doublet in the Soret region: the intensity of the negative band at 417 nm depends on heme–protein interactions [30] or, more exactly, on the distance and orientation of the phenylalanine residue positioned on the methionine side of the heme [33].

The presence of urea at high concentration (9 M) results in the overall simplification of the CD spectrum of cyt *c* at pH 7.0 (Fig. 3). The replacement of the 208 and 222 nm dichroic minima by a large negative minimum below 210 nm suggests the occurrence of a typical helix-to-random coil transition. The relatively complex dichroic pattern in the near-UV region of the CD spectrum is reduced to a single positive peak at about 258 nm. The Soret region shows a

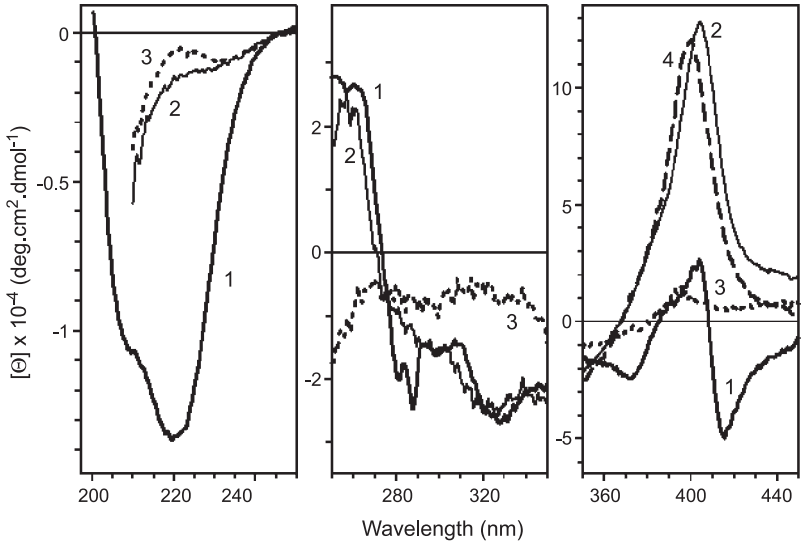

Fig. 3. CD spectra of ferric cyt *c* in 10 mM phosphate buffer: (thick solid line) in the absence of urea, pH 7.5; (thin solid line) 9 M urea, pH 7.5; (dotted line) 9 M urea, pH 2.5; (dashed line) 9 M urea, pH 5.1.

single positive peak at 404 nm indicating a disruption of the coupling between π→π* transitions of the heme group and those of the aromatic amino acid residues in its proximity. Acidification of the solution leads to further simplification of the CD spectrum for ferric cyt *c*. The maximum in the Soret region shifts from 404 nm (pH 7.0) to 400 nm at pH~5.0 without significant change in its intensity (Fig. 3). Similarly, no significant change was observed in the peptide region of CD spectrum (data not shown) indicating only small conformational change in the heme environment without a pronounced effect on the secondary structure of cyt *c*. Further lowering of the solution pH resulted in a nearly complete disappearance of the Soret CD peak accompanied by a slight shift of its maximum to ~395 nm. Analysis of the behavior of the Soret CD band gave a pK_a=3.8±0.1 and n=0.8±0.1 (data not shown). On the other hand, pH dependence followed at 258 and at 220 nm resulted in the pK_a and n values of 5.2±0.04, 0.9±0.1, and 4.1±0.3, 0.8±0.03, respectively. Since the difference between 0% and 100% at 220 nm was relatively small, to avoid possible errors in the determination of ellipticity at 220 nm due to slight baseline shifts, the differences in the signal recorded at 220 and 250 nm were taken instead. The variability in the pK_a values for the CD measurements at different wavelengths suggest that the changes in the secondary structure as well as tertiary structure of cyt *c* are not synchronized with the conformational changes taking place close to the heme of the ferric cyt *c*.

3.1.3. Electrochemistry

Cyt *c* was found to undergo a reversible one-electron redox process in 9 M urea on a 2-mercaptoethanol-modified Ag(111) electrode. Fig. 4 shows the important anodic shift (ca. 100 mV) of the formal redox potential ($E^{\circ\prime}$) for cyt *c* during the acidic titration in highly concentrated urea solution. A pK_a value of 5.1, obtained from the cyclic voltammetric experiment, correlates roughly with the protonation of His33 in cyt *c* and with the observed potential shift that follows the conversion of bis–His-ligated ferric cyt *c* to its high spin form (cf. Fig. 2). Cathodic-to-anodic peak separation was ca. 60 mV, typical of reversible one-electron transfer reaction (Nernstian behavior).

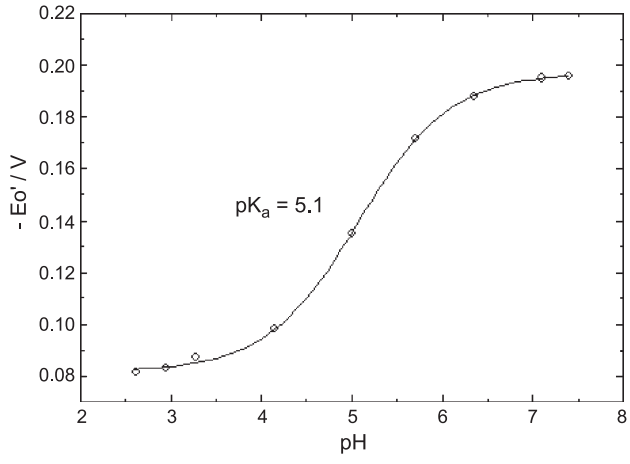

Fig. 4. Variation of the $E^{\circ\prime}$ potential for 1 mM cyt *c* during the acid/base titration in 9 M urea recorded on 2-mercaptoethanol-modified Ag(111) electrode. Scan rate: 100 mV/s.

3.1.4. Resonance Raman

The RR spectra reported in Fig. 5A show characteristic bands of a six-coordinate low spin ferric heme with His18 and Met80 as axial ligands. In the presence of urea, the frequencies of the core size marker bands increase. In 9 M urea, the spectrum becomes identical to that of bis–His cyt *c*″ at pH 7.0 [27] and resembles very closely that of ferric cyt *c* pH 5.9 in 4.4 M GdnHCl [11]. Therefore, the spectrum of ferric cyt *c* at pH 7.0 in 9 M urea is consistent with a bis–His coordinated form of the protein. The up-shift of the frequencies of the core size marker bands indicates a partial relaxation of the heme distortion toward a planar geometry [27,34] as compared to the native protein.

The RR spectrum of ferric cyt *c* in acidic solution of pH 2.0 (Fig. 5A, curve e) shows Raman shifts characteristic for a mixture of six-coordinate and five-coordinate high spin species [35]. The six-coordinate high spin ferric species is assigned to a His/H_2O complex of ferric cyt *c* with the native His18 ligand remaining coordinated to the heme, and the other His ligand is replaced by a water molecule. The five-coordinate high spin state corresponds to a species with a single axial ligand, which, in analogy with previous assignments, might be due either to His18 [10] or a water molecule (Ref. [33] and references therein). An increase of the six-coordinate high spin ferric heme is observed upon addition of 9 M urea, as judged by the appearance of 1484 cm^{-1} (ν_3) and 1615 cm^{-1} (ν_{10}) bands. The shoulders at 1490 cm^{-1} (ν_3) and 1622 cm^{-1} (ν_{10}) are assigned to the bands of the five-coordinate high spin heme. The spectrum resembles the spectrum of ferric cyt *c* at pH 4.0 in 4.4 M GdnHCl [11].

The low-frequency region (Fig. 5B) can furnish further information on the tertiary structure of ferric cyt *c* through the vibrations of the heme peripheral substituents and porphyrin out-of-plane modes. At neutral pH, ferric cyt *c* displays a very complex spectrum. In fact, due to the fairly distorted heme, many out-of-plane modes, normally not RR-active, become active [36]. Therefore, the spectrum should lose its complexity upon relaxation of the heme. A large intensity decrease and frequency changes of several bands can be observed. In particular, a decrease in the intensity is clearly evident for the bands at 445, 566, and 729 cm^{-1} assigned in horse heart cyt *c* to the out-of-plane modes γ_{22}, γ_{21}, and γ_5, respectively [36]. In addition, substantial intensity decrease is also observed for the vibration of the thioether linkages, specifically [$\delta(C_\beta C_a S)$] at 397 cm^{-1} and ν(C-S) at 692 cm^{-1}, although this latter band becomes overlapped with the down-shifted ν_7 vibration (observed at 699 cm^{-1}). These changes arise due to alteration of the thioether geometry in the presence of urea. Similar intensity

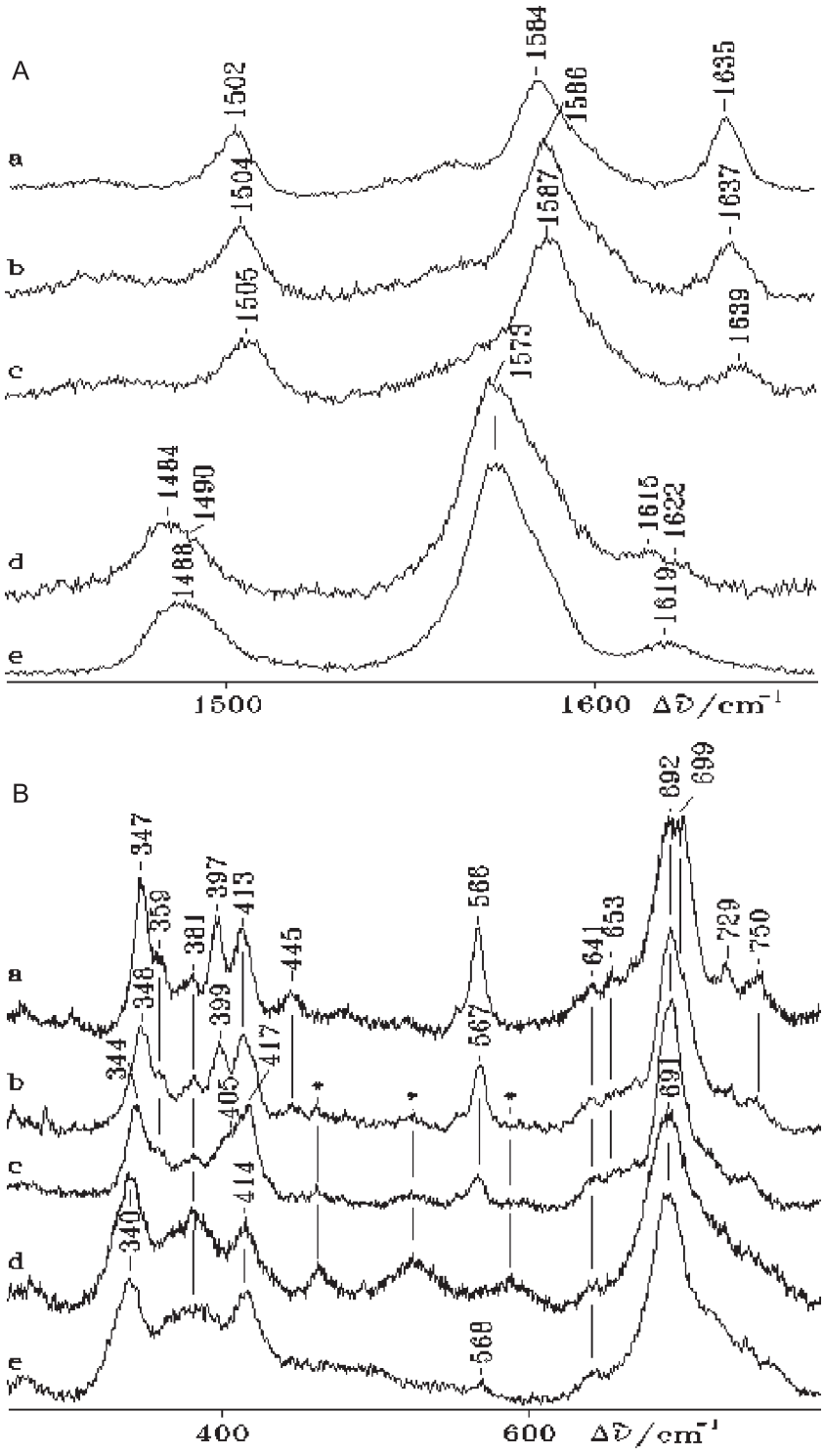

Fig. 5. (A) RR spectra of ferric cyt *c*, 406.7 nm excitation wavelength, 20 mW laser power at the sample; 5 cm^{-1} resolution; (a) pH 7.0, no urea, 11 s/0.5 cm^{-1} accumulation time; (b) pH 7.0, 6 M urea, 9 s/0.5 cm^{-1} accumulation time; (c) pH 7.0, 9 M, 9 s/0.5 cm^{-1} accumulation time; (d) pH 2.0, 9 M urea, 8 s/0.5 cm^{-1} accumulation time; (e) pH 2.0, no urea, 10 s/0.5 cm^{-1} accumulation time. (B) RR spectra of ferric cyt *c* in the low frequency region. Experimental conditions as in panel A. (a) pH 7.0, no urea, 3 s/0.5 cm^{-1} accumulation time; (b) pH 7.0, 6 M urea, 10 s/0.5 cm^{-1} accumulation time; (c) pH 7.0, 9 M, 11 s/0.5 cm^{-1} accumulation time; (d) pH 2.0, 9 M urea, 13 s/0.5 cm^{-1} accumulation time; (e) pH 2.0, no urea, 6 s/0.5 cm^{-1} accumulation time. The asterisks indicate the bands due to urea.

changes for the thioether bands have been observed in the RR spectrum of a ferric cyt *c* mutant in which Met80 has been replaced by cysteine, causing structural reorganization of the heme pocket [37]. The band at 397 cm^{-1} almost disappears with increasing urea concentration, while a new band at about 405 cm^{-1} appears. Based on the previous

results of the imidazole complex of ferric microperoxidase-8 [38] and cytochrome c'' [27], we assign the shoulder at 405 cm^{-1} to the asymmetric stretching mode [ν_{as}(Fe-Im_2)], which is predicted to be Raman-active if the ligands are inequivalent [39]. Therefore, these results suggest that at pH 7.0, 9 M urea causes the removal of the Met-80 ligand and the formation of a bis–His six-coordinate low spin ferric heme. The heme relaxes toward a planar geometry as a consequence of decreased protein contacts.

At pH 2, the low-frequency spectra of ferric cyt *c* with and without urea are very similar and the complex RR structure is completely lost. Upon addition of urea, the very weak γ_{21} band at 568 cm^{-1} completely disappears suggesting the absence of any heme-polypeptide contact. Kataoka et al. [40] considered the protein completely unfolded under these conditions. Some changes are also observed at 381 cm^{-1}, which may suggest differences in the hydrogen bonding between the propionyl groups and the surrounding protein.

3.1.5. MCD

In order to obtain more detailed information on the nature of the axial ligands, we investigated the urea-denatured ferric cyt *c* by MCD in the UV–vis and in the NIR regions (Fig. 6). In particular, bands in the latter region allow one to distinguish between bis–His and Met/His ligation in ferric low spin heme proteins [41]. The spectra of three ferric cyt *c* derivatives displayed in Fig. 6B, native cyt *c* (His/Met ligation), imidazole-ligated cyt *c* (His/Imid ligation), alkaline cyt *c* (His/Lys ligation) are all generally similar to the spectrum of urea-denatured cyt *c* at neutral pH. Of the four spectra, the intensities and band positions of the spectrum of alkaline ferric cyt *c* are the most different (over 40% larger peak-to-trough intensity in the Soret region and ~5 nm blue-shift in Soret cross-over wavelength), possibly indicating that neutral urea-denatured cyt *c* is not His/Lys-ligated.

To further narrow down the possible ligation states for ferric cyt *c* in 7 M urea at neutral pH, its NIR MCD spectrum was measured (Fig. 6A). The spectrum features a peak at 1545 nm and a shoulder at approximately 1300 nm. Also, in Fig. 6A are the spectra of a bis–His(Imid)-ligated species, ferric Imid-bound cyt *c* at neutral pH [41,42], and a Lys/His-ligated species, ferric cyt *c* at high pH (pH/pD=11.8) [41,42] with maxima of 1490 and 1480 nm and shoulders at 1270 and 1250 nm, respectively. The peak positions observed for Met/His-ligated species in the NIR region occur in the range from 1740 to 1860 nm [41]. The peak position of 1545 nm observed for ferric cyt *c* in 7 M urea neutral pH is well outside of this range. The spectrum of the bis–His-ligated species in Fig. 6A has a peak at 1490 nm with a shoulder at approximately 1270 nm. The range of peak positions observed in the NIR MCD spectra of all bis–His-ligated species occurs between 1455 and 1564 nm, a range that encompasses the peak position at 1545 nm observed for urea-denatured ferric cyt *c*. This range also overlaps the peak position at 1480 nm observed for a Lys/His-ligated species, ferric cyt *c* at high pH (Fig. 6B). From the NIR MCD data alone, Met/His ligation of ferric cyt *c* at neutral pH in the presence of 7 M urea can be ruled out, but it cannot be determined whether this derivative is bis–His- or Lys/His-ligated. When all of the available data including the RR as well as UV–vis and NIR MCD spectra are taken together, however, it can be concluded that the urea-denatured protein at neutral pH is bis–His-ligated.

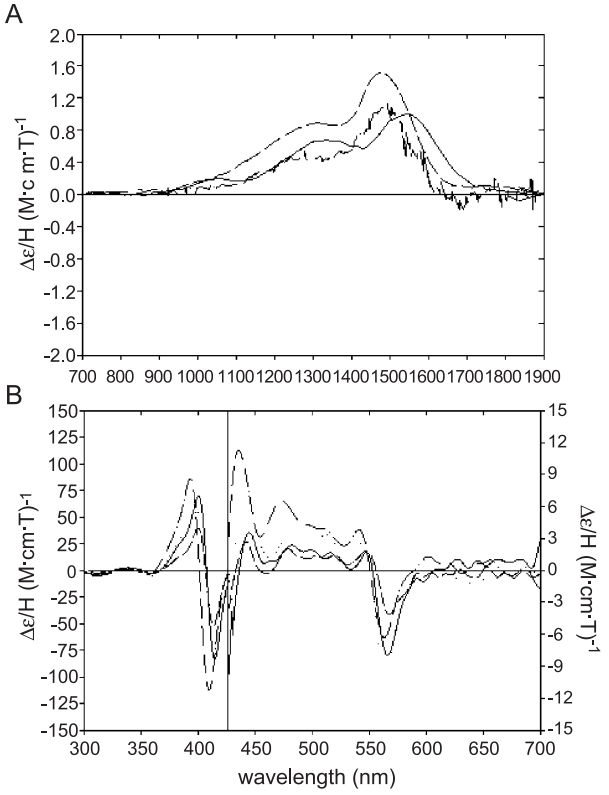

Fig. 6. (A) MCD of ferric imidazole-bound cyt *c* at pD 7, ferric denatured cyt *c* in urea at pD 7, and native ferric cyt *c* at pD 11.8 in the NIR region. Key for NIR spectra: (—) cyt *c* (4.28 mM) in 7 M urea, 10 mM KPi pD 7; (- - -) cyt *c* (3.08 mM) in 10 mM KPi pD 11.8; (-·-) cyt *c* (3.3 mM)+H-imidazole (9.0 M) in 10 mM KPi pD 7, replotted from data taken from Ref. [43]. (B) MCD of ferric cyt *c* in 7 M urea at pD 7, ferric imidazole-bound HH cyt *c* at pD 7, ferric cyt *c* at pD 7, and ferric cyt *c* at pD 11.8 in the UV–visible region. Key for UV–visible MCD spectra: (—) cyt *c* (66 μM) in 7.0 M urea, 10 mM KPi pD 7; (- - -) cyt *c* (50.1 μM) +2.5 M imidazole in 10 mM KPi pD 7; (-· ·-) cyt *c* (39 μM) in 10 mM KPi pD 7; (-·-) cyt *c* (57 μM) in 10 mM KPi pD 11.8.

The UV–vis MCD spectrum of ferric cyt *c* in 9 M urea at low pH is compared to that of ferric mesoporphyrin-reconstituted horse heart myoglobin (Fig. 7A) [43], which is a water/His-ligated species. Mesoporphyrin was used for this comparison because it has eight alkyl substituents (i.e., no vinyl substituents) as is the case for heme *c*. The close similarity between the two spectra suggests that the coordination structure of urea-denatured ferric cyt *c* at low pH consists of water/His ligation. This conclusion is supported by the similarity between the NIR MCD spectrum of acidic denatured cyt *c* to that of ferric myoglobin at neutral pH (water/His-ligated) (Fig. 7B) (because NIR MCD

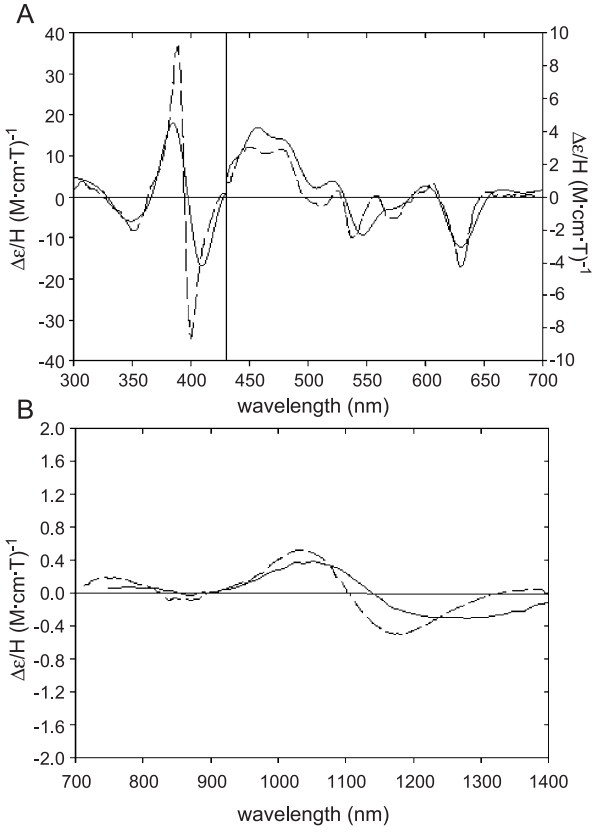

Fig. 7. (A) MCD of horse heart ferric cyt *c* in 9 M urea at pD 2 and ferric horse heart mesoporphyrin-reconstituted myoglobin in the UV–visible region: (—) cyt *c* (52 μM) in 9 M urea, 10 mM KPi pD 2; (- - -) mesoporphyrin reconstituted myoglobin (42 μM) in 100 mM KPi pD 7 (replotted from data in Ref. [44]). (B) MCD of ferric horse heart cyt *c* in 9 M urea at pD 2 and ferric horse heart myoglobin at pD 7 in the NIR region. NIR MCD spectra: (—) cyt *c* (2.06 mM) in 9 M urea, 10 mM KPi pD 2; (- - -) myoglobin (1.97 mM) in 50 mM KPi pD 7.

bands are much broader than those in the UV–visible region, it is not necessary to use mesoporphyrin-reconstituted myoglobin for this comparison). The similarity between the UV–vis and NIR MCD spectra of urea-denatured cyt *c* at low pH to the corresponding spectra of a His/water-ligated species argues that the axial ligands to the heme iron of the former are also His and water.

3.2. Spectroscopy of ferrous cytochrome c in urea

3.2.1. UV–vis absorption and CD

Native six-coordinate low spin ferrous cyt *c* is characterized by a red-shifted Soret absorption band at 415 nm and Q bands at 520 and 550 nm. As previously reported [29,30], at pH 7.0, no appreciable changes are observed in the overall spectrum upon addition of 9 M urea (Fig. 8, curves 1 and 2). However, at pH values below 5, dramatic changes are observed in the spectra. At pH 3.7 in 9 M urea, the Soret absorption band red-shifts by about 5–6 nm (data not shown) and the visible region is characterized by a broad absorption band with the maximum at 550 nm (Fig. 8, curve 3). These changes are characteristic of a five-coordinate high spin state of ferrous cyt *c* [44,45]. The apparent pK_a for the low spin to high spin state transition of ferrous cyt *c* is 4.8.

In agreement with the UV–vis absorption spectra, the CD spectrum of the ferrous protein in the Soret region differs significantly from that of the ferric protein (Fig. 9A). The major positive peak in the Soret region is at about 425 nm instead of 404 nm as in the case of ferric cyt *c*. In the near-UV region, the CD spectrum is characterized by a positive band centered around 251 nm and a negative band at 325 nm. The 2–3-fold increase in the ellipticity of the peak at 251 nm upon reduction of the protein obscures almost all of the other dichroic bands [30]. The change in redox state of the protein resulted in changes in the sign of dichroic bands at 282 and 288 nm, which tends to indicate a possible change in asymmetry of the Trp-59 in ferrous cyt *c* [30]. On the other hand, shoulders at 250, 287 and 300 nm suggest that the number of ellipticity bands upon reduction of cyt *c* is unchanged.

Only minor changes in the CD spectra were observed for ferrous cyt *c* at pH 7 in the presence of 9 M urea, consistent with the relatively small changes observed in the UV–vis absorption spectra. A slight (~10%) decrease in ellipticity of ferrous cyt *c* at 222 nm and minor changes in the aromatic and Soret regions of CD spectrum are noted. As in the case of ferric cyt *c*, acidification of the ferrous cyt *c* solution in 9 M urea leads to an overall simplification of CD spectrum. The intensity changes in the ellipticity of the various bands induced by acidification of the solution are shown in Fig. 9B. The intensity of the 425 nm band in the Soret region decreased with an apparent pK_a 5.0 and n 1.08. The intensity changes of the bands at 262 and 222 nm gave pK_a values of 5.32 and 5.12 and n values of 0.84 and 0.91, respectively. Interestingly, in contrast to ferric cyt *c*, a single pH-dependent transition of protein conformation with an apparent p$K_a \approx 5.15$ with consumption of one proton was observed. Despite the similar pK_a values observed for the first pH-transition of both ferrous and ferric cyt *c*, in the

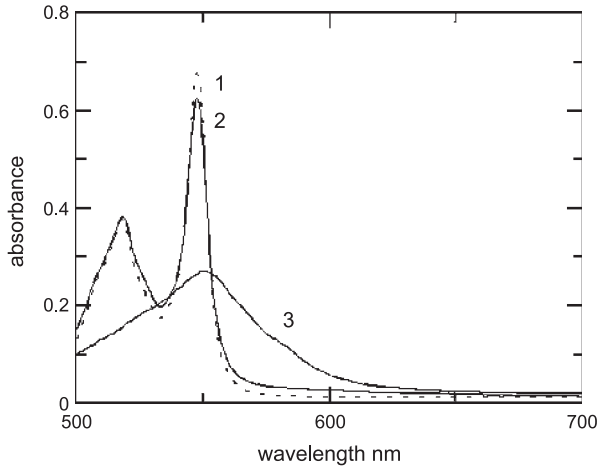

Fig. 8. UV–vis absorption spectra of ferrous cyt *c* at different pHs. Curve 1—pH 7.0; 2—pH 7.0, urea 9 M; 3—pH 3.7, urea 9 M.

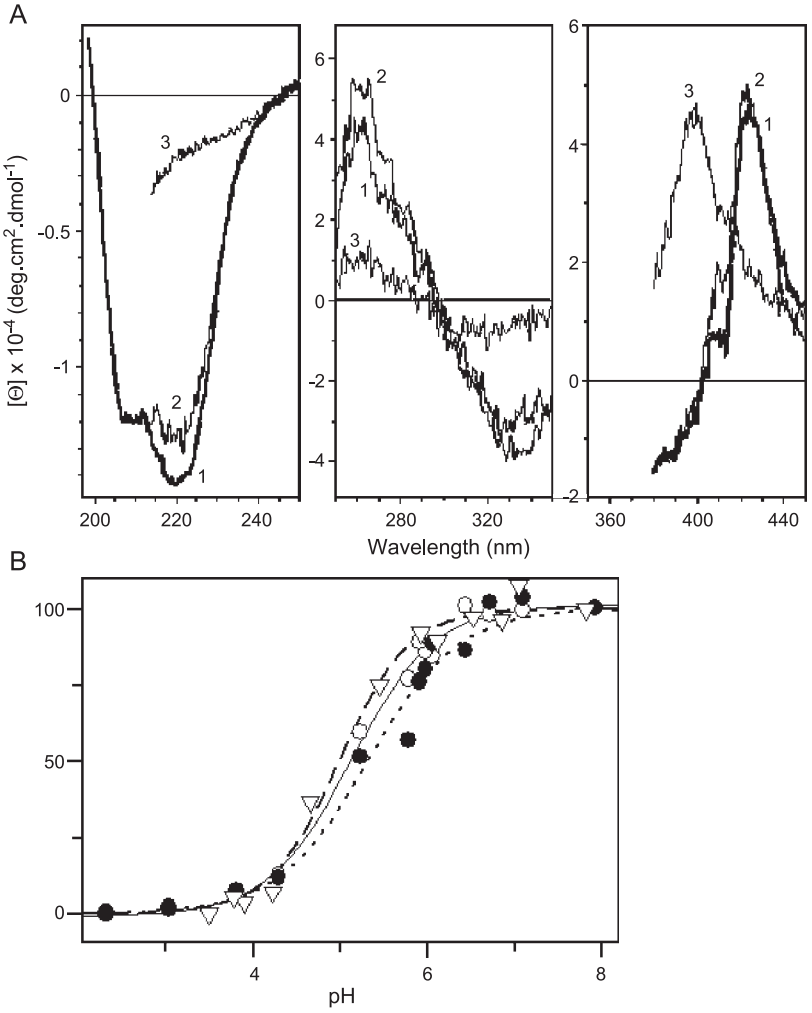

Fig. 9. (A) CD spectra of ferrous cyt *c* in 10 mM phosphate: pH 7.5, no urea (spectrum 1); pH 7.5, 9 M urea (2); pH 4.0, 9 M urea (3).(B) pH dependence of the ellipticity of the CD bands of ferrous cyt *c* in 9 M urea: (Λ) 425 nm; (●) 258 nm; (○) 222 nm.

case of the ferrous protein there is a direct transition from the six coordinate His/Met(His18–Fe–Met80) ligation to a five coordinate His-ligated state. This contrasts to the conversion of His/Met to bis–His-ligation (at pH 7) and then to His/Water-ligation (upon acidification) as observed for ferric cyt *c*. This is in accordance (i) with ~500-fold higher intrinsic affinity of Met80 for the ferrous versus ferric heme [11], (ii) the basically unaffected CD spectrum for ferrous cyt *c* in the presence of 9 M urea at pH 7 (Fig. 9A), and (iii) the decreased affinity of protonated imidazole of histidines towards heme-ligation [45]. Below pH~4.0, the UV–vis absorption spectra show dramatic changes (data not shown) and a transition from a five coordinate state to another conformational form is suggested.

3.2.2. MCD

The UV–vis MCD spectrum of ferrous cyt *c* in 7–9 M urea at neutral pH is consistent with retention of Met/His ligation as found in the native protein. In fact, as can be seen in Fig. 10, the spectrum of the protein at neutral pH is very similar to that of native ferrous cyt *c* at neutral pH (Met/His ligation). In contrast, the spectrum of the bis-imidazole(Im)-ligated octa-ethylporphyrin (OEP) model compound [46], Fe^{2+}(OEP) (N-MeIm$_2$) (data not shown) is sufficiently different, especially in the Soret region where the predom-

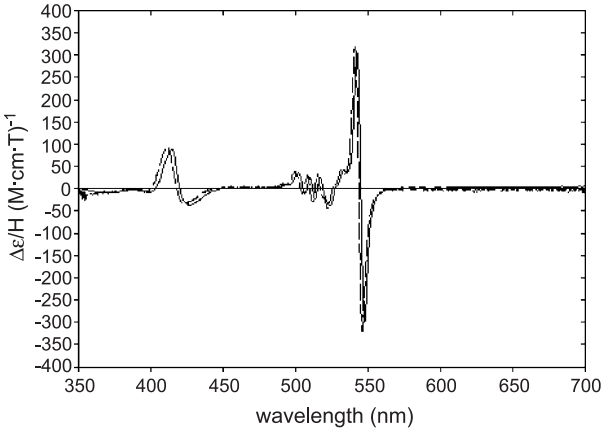

Fig 10. MCD of ferrous cyt *c* in the UV–visible region. (—) 40.0 μM, in 7 M urea, 10 mM KPi, pD 7; (- - -) 18.4 μM, in 10 mM KPi, pD 7.

inantly derivative-shaped pattern is of opposite sign (peak then trough with decreasing wavelength).

Upon lowering the pH to 4.5, the spectrum of ferrous cyt *c* remains generally unchanged, suggesting that the coordination environment remains His/Met-ligation. Changes in the UV–vis and MCD spectra of ferrous cyt *c* were observed below pH 4.5. In addition, the increased turbidity of the acidic dithionite solution and partial heme oxidation did not allow detailed characterization of the heme ligation state below pH 4.5. Further decreases in solution pH (pH 2–3) lead to irreversible changes in the MCD spectrum of ferrous cyt *c* until at pH 2 (data not shown), the spectrum does not resemble that of any known species, protein or model, and therefore the classification of the ligation state cannot be determined.

The present work clearly shows that depending on the urea concentration and solution pH, the unfolding of cyt *c* is accompanied by heme iron ligand-exchange reactions and important conformational changes of the protein. Through the combination of RR as well as MCD spectroscopy, it is shown that ferric cyt *c* in 7–9 M urea at neutral pH has a bis–His ligation structure. Under acidic conditions, direct experimental evidence from MCD spectroscopy has been obtained for the first time for the formation of a His/H_2O–Fe(III) complex of urea-denatured ferric cyt *c*. This is quite different from the five-coordinate aquo complex of ferric cyt *c* reported in acidic 6 M GdnHCl solution of pH 2–3 [28].

The acid titration of ferric cyt *c* in 9 M urea was accompanied by a color change from red to dark green. This is attributed to a low-to-high spin transition of cyt *c*, in which the protein adopts a His/H_2O axial coordination, which is shown to retain its electrochemical activity. On the other hand, the acidification of cyt *c* solution to pH<3 in the absence of urea led to a complete loss of the electron exchange between the mercaptoethanol-modified gold, or silver electrodes. The acidic titration of ferric cyt *c* in 9 M urea measured by cyclic voltammetry gave a pK_a value of 5.1, essentially identical to the pK of 5.2 determined spectrally. The experimental evidence obtained by RR and MCD suggests that the protonation of His33 triggers formation of the high spin His/H_2O complex of ferric cyt *c*. The fact that the His33—rather than His26 is the dominant sixth heme ligand under denaturating conditions (GdnHCl) was reported by Colon et al. [47], who compared the acidic titration of both histidines with that of corresponding Gln and Asn mutants, respectively.

The pK_a of 4.8 for the acid transition of ferrous cyt in 9 M urea is somewhat lower than for the ferric form of the protein. At neutral pH, the urea-denatured ferrous protein has been shown to retain its Met/His coordination structure. Below the pK_a, the urea-denatured ferrous protein converts to a five-coordinate high spin state of undetermined coordination structure.

In summary, through the combined use of several spectroscopic techniques as well as electrochemistry, the heme iron coordination of unfolded ferric and ferrous cytochrome *c* in neutral and acidic urea solutions has been established. Assignment of the spin state and axial ligation of the heme iron in the unfolded protein provides new insights that will be of importance to ongoing investigations of cytochrome *c* folding and unfolding.

Acknowledgements

This research was funded in part by grants from MIUR (COFIN 2001031798) (to G.S.), VEGA 3198 (to M.A.), and NIH GM 26730 (to J.H.D.).

References

[1] X. Liu, C.N. Kim, J. Yang, R. Jemmerson, X. Wang, Induction of apoptotic program in cell-free extracts: requirement for dATP and cytochrome *c*, Cell 86 (1996) 147–157.
[2] A. Gross, J.M. McDonnell, S.J. Korsmeyer, BCL-2 family members and the mitochondria in apoptosis, Genes Dev. 13 (1999) 1899–1911.
[3] S.H. Kaufmann, M.O. Hengartner, Programmed cell death: alive and well in the new millennium, Trends Cell Biol. 11 (2001) 526–534.
[4] S.B. Prusiner, Prions, Proc. Natl. Acad. Sci. U. S. A. 95 (1998) 13363–13383.
[5] D.A. Debe, M.J. Carlson, W.A. Goddard III, The topomer-sampling model of protein folding, Proc. Natl. Acad. Sci. U. S. A. 96 (1999) 2596–2601.
[6] J.D. Bryngelson, J.N. Onuchic, N.D. Socci, P.G. Wolynes, Funnels, pathways, and the energy landscape of protein folding: a synthesis, Proteins 21 (1995) 167–195.
[7] C.M. Dobson, A. Sali, M. Karplus, Protein folding: a perspective from theory and experiment, Angew. Chem., Int. Ed. 37 (1998) 868–893.
[8] C.M. Dobson, M. Karplus, The fundamentals of protein folding: bringing together theory and experiment, Curr. Opin. Struck. Biol. 9 (1999) 92–101.
[9] W. Colon, H. Roder, Kinetic intermediates in the formation of the cytochrome *c* molten globule, Nat. Struct. Biol. 3 (1996) 1019–1025.
[10] S. Takahashi, S.-R. Yeh, T.K. Das, C.-K. Chan, D.S. Gottfried, D.L. Rousseau, Folding of cytochrome *c* initiated by submillisecond mixing, Nat. Struct. Biol. 4 (1997) 44–50.
[11] S.R. Yeh, S. Takahashi, B. Fan, D.L. Rousseau, Ligand exchange during cytochrome *c* folding, Nat. Struct. Biol. 4 (1997) 51–56.
[12] S.R. Yeh, D.L. Rousseau, Folding intermediates in cytochrome *c*, Nat. Struct. Biol. 5 (1998) 222–228.
[13] Y. Xu, L. Mayne, S.W. Englander, Evidence for an unfolding and refolding pathway in cytochrome *c*, Nat. Struct. Biol. 5 (1998) 774–778.
[14] B.S. Russell, R. Melenkivitz, K.L. Bren, NMR investigation of ferricytochrome *c* unfolding: detection of an equilibrium unfolding intermediate and residual structure in the denatured state, Proc. Natl. Acad. Sci. U. S. A. 97 (2000) 8312–8317.
[15] B.S. Russell, K.L. Bren, Denaturant dependence of equilibrium unfolding intermediates and denatured state structure of horse ferricytochrome *c*, J. Biol. Inorg. Chem. 7 (2002) 909–916.
[16] S. Akiyama, S. Takahashi, K. Ishimori, I. Morishima, Stepwise formation of alpha-helices during cytochrome *c* folding, Nat. Struct. Biol. 7 (2000) 514–520.
[17] A. Caflisch, M. Karplus, Structural details of urea binding to barnase: a molecular dynamics analysis, Struct. Fold. Des. 5 (1999) 477–488.
[18] J. Cheek, J.H. Dawson, Magnetic circular dichroism spectroscopy of heme iron systems, in: K. Kadish, K. Smith, R. Guilard (Eds.), Handbook of Porphyrins and Related Macrocycles, vol. 7, Academic Press, New York, 2000, pp. 339–369.

[19] G. Smulevich, Understanding heme cavity structure of peroxidases: comparison of electronic absorption and resonance Raman spectra with crystallographic results, Biospectroscopy 4 (5 Suppl.) (1998) S3–S17.
[20] E. Margoliash, N. Frohwirt, Spectrum of horse heart cytochrome *c*, Biochem. J. 71 (1959) 570–572.
[21] K.M. Smith (Ed.), Porphyrins and Metalloporphyrins, Elsevier Scientific Publishing, Amsterdam, 1975, pp. 804–807.
[22] C.N. Pace, Determination and analysis of urea and guanidine hydrochloride denaturation curves, Methods Enzymol. 131 (1986) 266–280.
[23] D.G. Reid, L.K. MacLachlan, A.J. Edwards, J.A. Hubbard, P.J. Sweeney, Introduction to the NMR of proteins, Methods Mol. Biol. 60 (1997) 1–28.
[24] J.J. Rux, Magnetic circular dichroism studies of chloroperoxidase, cytochrome P450, cytochrome *c* and related heme proteins, PhD thesis, University of South Carolina, 1991, Chapter 4.
[25] N. Sutin, J.K. Yandell, Mechanisms of the reactions of cytochrome *c*. Rate and equilibrium constants for ligand binding to horse heart ferricytochrome *c*, J. Biol. Chem. 247 (1972) 6932–6936.
[26] A. Schejter, I. Aviram, The reaction of cytochrome *c* with imidazole, Biochemistry 8 (1969) 149–153.
[27] C. Indiani, G. De Sanctis, F. Neri, H. Santos, G. Smulevich, M. Coletta, Effect of pH on axial ligand coordination of cytochrome *c″* from *Methylophilus methylotrophus* and horse heart cytochrome *c*, Biochemistry 39 (2000) 8234–8242.
[28] S.R. Yeh, S.W. Han, D.L. Rousseau, Cytochrome *c* folding and unfolding: a biphasic mechanism, Acc. Chem. Res. 31 (1998) 727–736.
[29] D.W. Urry, The heme chromophore in the ultraviolet, J. Biol. Chem. 242 (1967) 4441–4448.
[30] Y.P. Myer, Conformation of cytochromes: II. Comparative study of circular dichroism spectra, optical rotatory dispersion, and absorption spectra of horse heart cytochrome *c*, J. Biol. Chem. 243 (1968) 2115–2122.
[31] Y.P. Myer, Conformation of cytochromes: 3. Effect of urea, temperature, extrinsic ligands, and pH variation on the conformation of horse heart ferricytochrome *c*, Biochemistry 7 (1968) 765–776.
[32] A.M. Davies, J.G. Guillemette, M. Smith, C. Greenwood, A.G.P. Thurgood, A.G. Mauk, G.R. Moore, Redesign of the interior hydrophilic region of mitochondrial cytochrome *c* by site-directed mutagenesis, Biochemistry 32 (1993) 5431–5435.
[33] G.J. Pielak, K. Oikawa, A.G. Mauk, M. Smith, M.K. Cyril, Elimination of the negative Soret Cotton effect of cytochrome *c* by replacement of the invariant phenylalanine using site-directed mutagenesis, J. Am. Chem. Soc. 108 (1986) 2724–2727.
[34] L.S. Sparks, K.K. Anderson, C.S. Medforth, K.M. Smith, J.A. Shelnutt, Correlations between Raman frequencies and structure for planar and nonplanar metalloporphyrins, Inorg. Chem. 33 (1994) 2297–2302.
[35] S. Oellerich, H. Wackerbarath, P. Hildebrandt, Spectroscopic characterization of nonnative conformational states of cytochrome *c*, J. Phys. Chem., B 106 (2002) 6566–6580.
[36] S. Hu, J.K. Morris, J.P. Singh, K.M. Smith, T.G. Spiro, Complete assignment of cytochrome *c* resonance Raman spectra via enzymatic reconstitution with isotopically labeled hemes, J. Am. Chem. Soc. 115 (1993) 12446–12458.
[37] G. Smulevich, M.S. Bjerrum, H.B. Gray, T.G. Spiro, Resonance Raman-spectra and the active-site structure of semisynthetic Met80Cys horse heart cytochrome *c*, Inorg. Chem. 33 (1994) 4629–4634.
[38] S. Othman, A. Le Lirzin, A. Desbois, Resonance Raman investigation of imidazole and imidazolate complexes of microperoxidase: characterization of the bis(histidine) axial ligation in *c*-type cytochromes, Biochemistry 33 (1994) 15437–15448.
[39] T.G. Spiro, X.Y. Li, Resonance Raman spectroscopy of metalloporphyrins, in: T.G. Spiro (Ed.), Biological Applications of Raman Spectroscopy, Wiley-Interscience, New York, 1988, pp. 1–37.
[40] M. Kataoka, Y. Hagihara, K. Mihara, Y. Goto, Molten globule of cytochrome *c* studied by small angle X-ray scattering, J. Mol. Biol. 229 (1993) 591–596.
[41] P.M.A. Gadsby, A.J. Thomson, Assignment of the axial ligands of ferric ion in low-spin hemoproteins by near-infrared magnetic circular dichroism and electron paramagnetic resonance spectroscopy, J. Am. Chem. Soc. 112 (1990) 5003–5011.
[42] J.J. Rux, Magnetic circular dichroism studies of chloroperoxidase, cytochrome P450, cytochrome *c* and related heme proteins, PhD thesis, University of South Carolina, 1991, Chapter 2.
[43] J.H. Dawson, S. Kadkhodayan, C. Zhuang, M. Sono, On the use of iron octa-alkylporphyrins as models for protoporphyrin IX-containing heme systems in studies employing magnetic circular dichroism spectroscopy, J. Inorg. Biochem. 45 (1992) 179–192.
[44] C.M. Jones, E.R. Henry, Y. Hu, C.-K. Chan, S.D. Luck, A. Bhuyan, H. Roder, J. Hofrichter, W.A. Eaton, Fast events in protein folding initiated by nanosecond laser photolysis, Proc. Natl. Acad. Sci. U. S. A. 90 (1993) 11860–11864.
[45] A.K. Bhuyan, J.B. Udgaonkar, Folding of horse cytochrome *c* in the reduced state, J. Mol. Biol. 312 (2001) 135–1160.
[46] E.W. Svastits, J.H. Dawson, Models for ferrous cytochrome b_5: sign inversions in the magnetic circular dichroism spectra of bis-imidazole ferrous porphyrin systems, Inorg. Chim. Acta 123 (1986) 83–86.
[47] W. Colon, L.P. Wakem, F. Sherman, H. Roder, Identification of the predominant non-native histidine ligand in unfolded cytochrome *c*, Biochemistry 36 (1997) 12535–12541.